### Accepted Manuscript

Characterization of helium release from apatite by continuous ramped heating

Bruce D. Idleman, Peter K. Zeitler, Kalin T. McDannell

PII: S0009-2541(17)30640-X

DOI: doi:10.1016/j.chemgeo.2017.11.019

Reference: CHEMGE 18547

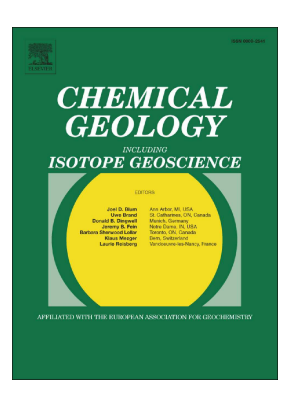
To appear in: Chemical Geology

Received date: 12 June 2017

Revised date: 14 November 2017 Accepted date: 15 November 2017

Please cite this article as: Bruce D. Idleman, Peter K. Zeitler, Kalin T. McDannell, Characterization of helium release from apatite by continuous ramped heating. The address for the corresponding author was captured as affiliation for all authors. Please check if appropriate. Chemge(2017), doi:10.1016/j.chemgeo.2017.11.019

This is a PDF file of an unedited manuscript that has been accepted for publication. As a service to our customers we are providing this early version of the manuscript. The manuscript will undergo copyediting, typesetting, and review of the resulting proof before it is published in its final form. Please note that during the production process errors may be discovered which could affect the content, and all legal disclaimers that apply to the journal pertain.



# Characterization of helium release from apatite by continuous ramped heating

Bruce D. Idleman<sup>a\*</sup>, Peter K. Zeitler<sup>a</sup>, and Kalin T. McDannell<sup>a, b</sup>

<sup>a</sup>Department of Earth and Environmental Sciences, Lehigh University, Bethlehem, PA 18015, USA

<sup>b</sup>Geological Survey of Canada, 3303 – 33 Street NW, Calgary, Alberta T2L 2A7, Canada

\*Corresponding author: bdi2@lehigh.edu

### **ABSTRACT**

Knowledge of the kinetic behavior of He in apatite and other U- and Th-bearing minerals comes largely from detailed step-heating experiments, yet such experiments are time consuming and are rarely performed during routine thermochronological studies using the U-Th/He method. We propose a new analytical method for measuring both the bulk <sup>4</sup>He abundance and the kinetics of He release in apatite. Using this method He is extracted from samples by continuous heating using a ramped temperature schedule under static vacuum conditions, and the evolved He is measured periodically as it accumulates in the extraction system. Continuous ramped heating (CRH) experiments can be conducted using instrumentation available in most noble-gas thermochronology labs but require particular attention to temperature control, measurement linearity and dynamic range, and suppression of active gases co-evolved with He. CRH experiments require little more time than conventional single-step heating measurements but yield a detailed record of He release not provided by conventional methods. Kinetic parameters for He diffusion in Durango apatite derived from continuous heating data agree well with those obtained from published step-heating studies. The continuous record of He release obtained from CRH experiments also provides important information about the siting of He and the presence of multiple He components in apatite, some of which may be responsible for anomalous U-Th/He ages and high age dispersion. As such the CRH method shows promise as a useful sample screening tool for apatite U-Th/He thermochronology.

**Keywords:** Apatite, diffusion, helium, mass spectrometry, thermochronology.

#### 1. Introduction

Dating of apatite by the U-Th/He method (Zeitler, 1987) has emerged as an important tool in the earth sciences. With its relatively low closure temperature for He diffusion of ~65°C (Shuster et al, 2006), apatite is capable of providing important constraints on timing of surface processes and the thermal evolution of the shallow crust. Current understanding of the retention and release of He in apatite has come largely from *in vacuo* step-heating experiments performed on commonly analyzed standards and a limited selection of unknown samples (Zeitler, 1987; Warnock et al., 1997; Wolf et al., 1996; Farley, 2000; Shuster et al., 2006). In addition to providing fundamental kinetic constraints for He loss by volume diffusion, these studies identified additional complicating factors that influence He retention and release in apatite, most notably the effects of lattice defects caused by radiation damage. Through experiments involving laboratory outgassing of radiogenic <sup>4</sup>He and proton-induced <sup>3</sup>He, Shuster et al. (2006) demonstrated that structural defects in apatite imparted by radiation damage from U and Th decay act to impede He diffusion. This observation led to the development of quantitative models relating radiation damage and He retentivity (e.g., Flowers et al., 2009; Gautheron et al., 2009; Willett et al., 2017) that have been successful at explaining at least some of the observed dispersion in apatite U-Th/He ages.

Despite this progress, there is growing recognition that some samples, particularly those from slowly cooled terranes, yield highly dispersed and/or geologically unreasonable apatite U-Th/He ages that are not readily explained by radiation-damage models (e.g., Fitzgerald et al., 2006; Flowers and Kelley, 2011; McKeon et al., 2014). Other factors implicated in the corruption of U-Th/He ages include U and Th-bearing inclusions (Farley, 2002; Vermeesch et al., 2007), trapping by a wide range of structural defects not related to radiation damage (Gerin et al., 2017; Zeitler et al., 2017), U and Th zoning (Farley et al., 2011), and implantation of He from external sources (Spiegel et al., 2009; Gautheron et al., 2012; Murray et al., 2014). All of these phenomena are predicted to modify the expected spatial distribution of He within grains in a variety of ways. Therefore, knowledge of the He distributions and release kinetics in affected samples is essential for identifying the factors that contribute to age dispersion and, ideally, deriving corrections for sample ages. It is an unfortunate fact that the two-step (extraction/re-extraction) heating method commonly employed to quantify He abundance in routine U-Th/He studies reveals no information about He kinetics and distribution in grains, and

the dispersion of ages obtained from analysis of replicate grains provides only crude insight into the integrity of the U-Th/He system. Step-heating experiments are currently the method of choice for detailed sample characterization, but because they are time consuming and require careful control of sample temperature during heating they are rarely applied in routine dating studies.

In this paper we present an alternative experimental approach to characterizing He release from apatite that entails heating samples continuously using a ramped, rate-controlled temperature schedule. The evolved gas is allowed to accumulate in the extraction system and is measured periodically by a gas-source mass spectrometer held open to the extraction line but operated in the static mode. The continuous ramped heating (CRH) method we describe is similar in many respects to continuous heating strategies employed in a few early noble-gas diffusion studies (e.g., Gerling et al., 1963; Levskii, 1963). The method presents some unique analytical challenges beyond those imposed by traditional step-heating (see section 2.1), but we demonstrate that it is capable of providing a faithful record of He release from apatite grains over a wide range of temperatures. With careful temperature control, CRH experiments using wellbehaved samples yield kinetic parameters for <sup>4</sup>He diffusion in apatite that agree remarkably well with those obtained from detailed step-heating experiments (e.g., Farley, 2000). CRH is a timeefficient method, and complete diffusion experiments that provide useful kinetic information can be carried out in the time needed to complete just a few conventional heating steps. Perhaps more importantly, for some poorly behaved samples, details of gas-release patterns can be used to screen for problematic factors associated with dispersed U-Th/He ages.

For continuously heated apatites subjected to a temperature ramp, outgassing by volume diffusion results in distinctive sigmoidal cumulative loss curves and bell-shaped incremental loss curves (Fig. 1). The positions and overall forms of these curves in parameter space are controlled by the diffusion kinetics of the sample and the heating schedule. The curves are modified in subtle ways by many of the processes that have been shown to affect He distribution in apatite (e.g., alpha ejection, radiation damage, zoning), but in most cases their distinctive shapes are preserved. However, as we illustrate below, poorly behaved ("bad actor") apatite samples that show large single-grain U-Th/He age dispersion commonly yield loss profiles that have complex shapes and/or are displaced from those of other apatites analyzed under the same experimental

conditions. From these observations we suggest that the CRH method represents a promising tool for screening apatite samples for U-Th/He thermochronology.

#### 2. Methods

### 2.1 Technical considerations

Step heating has been employed for decades as the tool of choice for characterizing the diffusion of noble gases in minerals. A typical heating step involves application of ideally a square thermal pulse to the sample to release a fraction of the noble-gas species of interest, a period of cooling and purification during which the evolved gas is exposed to chemical getters and/or separated cryogenically, and expansion of the purified gas into a gas-source mass spectrometer for analysis. Depending upon the application, the gas may be spiked for isotope-dilution analysis during or after heating. In most modern noble-gas experiments, the sample is analyzed in the static mode to achieve high sensitivity. Changes in the abundances and isotope ratios of the various gas species that occur within the mass spectrometer during analysis are accommodated by regressing the measured peak heights back to the time of gas inlet.

Modern gas-source mass spectrometers are particularly good at performing isotopic abundance measurements on purified and carefully sized aliquots of noble gases. The step-heating method is well-suited to producing such aliquots, since temperature and heating duration can be varied to tailor gas release to the optimum measurement range of the mass spectrometer, and the distinct purification stage that typically follows sample heating helps insure efficient removal of active gas contaminants that might interfere with measurement of noble-gas species or otherwise adversely affect the operating environment in the instrument. The CRH method, which in our experiments involves continuous isotopic measurement of a reservoir of rapidly evolving and often impure gas, places unique and potentially challenging demands on analytical instrumentation and methodology. In the following sections we summarize these analytical challenges and present strategies for addressing them.

### 2.1.1 System blank and gas consumption rate

During CRH experiments the He blank accumulates continuously while the mass spectrometer and extraction system are isolated from their pumping systems, which for our experiments was a period of 30 to 75 minutes. Although the duration of static vacuum during typical CRH runs commonly exceeds that experienced during conventional single-step heating of apatite, He blanks are typically quite low in modern analytical systems used for U-Th/He dating, and in many cases they can be disregarded without adding significantly to the overall error budget. In a series of detailed apatite diffusion experiments lasting up to several weeks, Farley (2000) demonstrated that blanks rarely exceeded 2% of the evolved <sup>4</sup>He. Helium blanks during our CRH experiments were typically <1 fmole and comprised <0.5% of the total release. Of greater concern for CRH analysis is the blank contribution associated with the lowest-temperature portion of the heating ramp, which may comprise as much as 5-10% of the total <sup>4</sup>He released during the early portion of a CRH experiment (Fig. 2). Failure to account for the blank in this early portion of the release does not typically influence the form of He release curves significantly, but accurate blank corrections may be necessary when evaluating the low-temperature portion of the release to constrain kinetic parameters.

Additionally, He released from the sample is slowly consumed as He ions interact with surfaces within the mass spectrometer. The He consumption rate is generally quite low in the small quadrupole mass spectrometers commonly used for U-Th/He thermochronology, particularly when they are operated at low emission currents (Fig. 2). In our system the  $^4$ He consumption rate is a direct but often complex function of  $^4$ He partial pressure, typically reaching values of  $\sim 1 \times 10^{-17}$  moles/min by the end of CRH runs. Except for samples with unusually high He contents, gas consumption is generally a minor or insignificant effect.

### 2.1.2 Mass spectrometer dynamic range and linearity

Gas fractions released during the early stages of CRH experiments are typically very small, often close to or even below the mass spectrometer's detection limit for <sup>4</sup>He. However, in marked contrast with step-heating experiments, all of the sample gas is present and must be quantified at the end of a CRH experiment. Therefore, the range of <sup>4</sup>He partial pressures encountered is typically at least several times greater than that experienced during step-heating analyses, and in some cases it may be well over an order of magnitude greater. Such wide pressure ranges impose

challenging requirements for pressure linearity and small-signal measurement precision on mass spectrometers used for CRH analysis.

Fortunately, many small quadrupole mass spectrometers of the type commonly used for U-Th/He dating are designed for residual gas analysis in industrial processes, and these instruments typically exhibit both excellent He pressure linearity and a very wide measurement range. For example, the Pfeiffer Prisma quadrupole used for He measurements in our laboratory exhibits highly linear response over a <sup>4</sup>He pressure range of >10<sup>4</sup> (Fig. 3). Pressures encountered during typical CRH heating experiments using single apatite crystals usually fall entirely within the linear response range.

### 2.1.3 Temperature response and gas conductance

Data are recorded during CRH experiments in the form of two time series, with each record in each series consisting of measurements of He abundance or sample temperature, and elapsed time (depending upon the instrumentation employed the temperature series may be inferred from the temperature ramp rate rather than measured directly). Since both sample temperature and He abundance change continuously during CRH experiments, it is essential to insure that these series are well registered (i.e., both temperature and He abundance reflect the true state of the system at the recorded elapsed time). This is particularly important for the determination of kinetic parameters from the He release records. Potential sources of mismatch include slow dynamic response of the sample heating system, and delays in gas transfer and pressure equilibration in the extraction line and mass spectrometer.

Systems that use laser energy to heat low-mass samples, typically single crystals wrapped in metal foil, are very responsive and can provide accurate temperature tracking at heating rates of >100°C/min. On the other hand, double-vacuum resistance furnaces of the type commonly employed for noble-gas analysis of bulk samples have much greater heated mass and less efficient coupling between sample and heating element, especially at lower temperatures, restricting their use to slow heating rates.

Delays in equilibrating pressure within the extraction line and mass spectrometer also degrade the correlation between measured He abundance and elapsed time. Extraction lines with low

conductance may require time corrections to account for the slow transfer of gas between the sample and mass spectrometer. In our He extraction line, the time constant for pressure equilibration after the addition of small He aliquots to the extraction line is < 2 seconds over the range of He pressures typically encountered during CRH experiments. This short delay corresponds to an effective mismatch between the recorded sample temperature and He measurement of 1°C or less at typical heating rates, and is small enough to be ignored in most situations.

### 2.1.4 Contaminating gas species

During CRH experiments the need to simultaneously heat a sample and measure its released He renders chemical gettering of active gases and the use of cryogenic methods to separate He from other gas species relatively inefficient. The presence of active gas contaminants in the gas released from both the sample and the extraction system (blank) has several important implications for CRH experiments. First, sufficiently high partial pressures of hydrogen (and potentially other active gases) will cause pressure scattering in the mass spectrometer, significantly altering the effective <sup>4</sup>He sensitivity (e.g., Cowan et al, 1994). Additionally, Lieszkovszky et al. (1990) have shown that high partial pressures of hydrogen and some other gas species can temporarily alter the sensitivity of quadrupole mass spectrometers for up to several tens of hours, introducing a hysteresis in the relationship between He partial pressure and sensitivity. For these reasons it is important to monitor potential contaminating species continuously during CRH experiments and to use a consistent protocol for determining the sensitivity used for each sample. Reducing the temperature ramp rate also provides additional effective gettering time and may help to relieve these problems to some extent.

Additionally, hydrogen evolution from the sample and extraction system complicates the use of a <sup>3</sup>He spike to determine <sup>4</sup>He abundances by isotope dilution, since evolved HD interferes with the measurement of <sup>3</sup>He and cannot be resolved from it by low-resolution quadrupole mass spectrometers. Therefore, the usual method of quantifying <sup>4</sup>He by isotope dilution using a <sup>3</sup>He spike may prove unreliable or require difficult corrections for HD. The severity of this problem will depend upon the nature of the analyzed samples, the design and cleanliness of the extraction system, and the efficiency of hydrogen gettering or separation. An alternative method is to

determine <sup>4</sup>He manometrically (i.e., by peak-height comparison) using the instrumental sensitivity obtained by measuring calibrated aliquots of <sup>4</sup>He before and after sample analysis. In our laboratory we have found that this strategy provides results that agree with those of the isotope-dilution method to better than 1%.

In our experience, the use of laser heating rather than a resistance furnace greatly reduces the evolution of H and other gases during analysis, as the mass of heated metal where much of the hydrogen resides is considerably smaller during laser heating. Regardless, the effects of contaminating gas species on analysis quality are generally of concern only for He measurements made during the active temperature ramp portion of CRH experiments. If an isotope dilution measurement of the total <sup>4</sup>He abundance is desired in order to calculate a sample's apparent age, the accumulated sample gas can be gettered or purified cryogenically and analyzed using conventional isotope dilution methods once heating has been completed.

### 2.1.5 Susceptibility to vacuum failure

The potential for vacuum failure during analysis that may lead to contamination or even failure of the mass spectrometer is of particular concern during CRH experiments, since a direct connection must be maintained between the sample and the mass spectrometer as the sample is heated to high temperature. Failure of the vacuum system places the mass spectrometer filament and detector at considerable risk. For modern all-metal ultra-high vacuum extraction lines that are held at static conditions, the risk of a spontaneous and catastrophic vacuum accident caused by the failure of valves, vacuum connections, etc. is probably quite small. Similarly, modern jacketed vacuum furnaces of the type commonly employed in noble-gas experiments are well protected by virtue of their double-walled design. However, viewports in laser chambers are particularly vulnerable to failure. For experiments employing laser heating, differentially pumped viewports and strongly convergent laser beams that minimize power density on the viewport window should provide some measure of protection from vacuum failure.

### 2.2 Materials

Our initial CRH experiments were performed using Durango apatite (Young et al., 1969), a quickly cooled, gem-quality fluorapatite associated with iron deposits at Cerro de Mercado near

Durango City, Mexico. Durango apatite is somewhat atypical with respect to most apatite samples dated using the U-Th/He method, having an unusually high Th/U of ~20 and high effective uranium content (eU) of ~50 ppm (eU = U + 0.235\*Th) (Flowers et al., 2009). However, it is widely used as a laboratory age and kinetic standard, and its diffusion behavior has been well characterized by conventional step-heating analysis (Zeitler et al., 1987; Wolf et al., 1996; Farley, 2000). The age of the Durango deposit has been determined to be 31.44  $\pm$  0.18 Ma by  $^{40}$ Ar/ $^{39}$ Ar ages from bounding ignimbrite deposits (McDowell, 2005). Samples for our CRH experiments were obtained from a single large Durango crystal from which the outermost region (~50  $\mu$ m) was first removed by grinding to eliminate portions of the crystal affected by alpha ejection (Farley et al., 1996). The crystal was then crushed and sieved to 180-250  $\mu$ m size, and sub-equant shards that appeared optically clear and inclusion-free under observation with a binocular microscope in air at 95x magnification were selected for analysis.

We also present results of CRH experiments on whole apatite single crystals from samples that exhibit strongly contrasting U-Th/He behavior in order to demonstrate the efficacy of the method as a sample screening tool for routine U-Th/He thermochronology. Sample 14MN07 was obtained from granite collected in the Orkhon River basin near Tsetserleg, Mongolia. Two optically clear, inclusion-free apatite crystals with sphere-equivalent diameters ( $2R_s$ ) of  $\sim 110~\mu m$  and eU  $\sim 27$  ppm were selected from this presumably slowly cooled granite. Both crystals yielded similar U-Th/He ages and showed simple He release behavior. Samples NB07 and NB54 were obtained from gneisses collected near Namche Barwa along the eastern syntaxis of the Himalayas in Tibet (Zeitler et al., 2014). Apatites from both of these samples are of excellent optical quality based upon microscopic examination, but they exhibit high age dispersion and unrealistically old ages when analyzed by the conventional U-Th/He method. Crystals selected for analysis from NB07 had eU concentrations of  $\sim 40$  ppm and spanned a size range of 74-114  $\mu$ m ( $2R_s$ ), while those from NB54 had 90-160  $\mu$ m equivalent diameters and averaged  $\sim 15$  ppm eU.

### 2.3 Instrumentation and Analytical Methods

Single apatite crystals selected for analysis were loaded into 0.7 mm outside diameter x 0.4mm long Nb tubes under a binocular microscope, and the ends of the tubes were crimped closed with

tweezers. For laser-heated samples we inserted short pairs of 0.13 mm type K thermocouple wire into opposite ends of the tubes prior to crimping. The contacts between the wire and Nb tube together form a thermocouple junction that was used to monitor sample temperature. The crimped tubes were then inserted into flat 2 mm x 2 mm packets folded from 0.015 mm Nb foil. These packets provide a flat surface that can be marked to allow identification of samples dropped sequentially during furnace analyses, and for laser heating analyses they present a smooth, flat surface to the defocused laser beam.

Helium extraction and analyses were performed using an all-metal ultra-high vacuum extraction line connected to a Pfeiffer Prisma QMS 200 quadrupole mass spectrometer. Sample heating was accomplished using either a double-vacuum resistance furnace or a fiber-coupled diode laser system. For the furnace heating experiments, the furnace temperature was monitored at the base of the molybdenum sample crucible using a W-Re thermocouple, and the temperature was controlled by a Eurotherm 2400 closed-loop controller that allows user control of starting temperature, ramp rate, and heating duration. This system uses a secondary Mo liner at the base of the crucible to allow for easy removal of samples. The laser system consists of an Ostech 30 watt 808 nm diode laser coupled by fiber-optic cable to a beam expander attached to a custom beam delivery system. Using a series of dichroic mirrors and filters, this system allows 808 nm laser light to be focused through a sapphire viewport onto the sample, while visible and longerwavelength infrared light are directed back along the beam axis to a video camera and BASF Exactus optical pyrometer, respectively. Sample temperature can be monitored and controlled using either type K thermocouples embedded in the sample packets or via the output signal of the optical pyrometer. The pyrometer simplifies the experimental setup by eliminating the need for embedded thermocouples, but it is inherently less precise and is influenced by variations in packet emissivity and orientation. In order provide the most reliable assessment of He diffusion kinetics, the laser-heating experiments described in section 3 were performed using thermocouple temperature monitoring. The pyrometer and linearized thermocouple outputs were sampled every 50 ms to help minimize small temperature excursions caused by fluctuations in laser beam intensity and changes in coupling efficiency between the beam and sample packet during heating. A custom Labview program modulated the laser power to provide closed-loop PID control of sample temperature, and allowed user control of ramp rate and other experimental parameters.

We used linear temperature ramps for our heating experiments, but it should be noted that heating schedules that employ multiple linear segments with differing rates, as well as those that are non-linear, will produce results broadly similar to those obtained from linear heating. A potentially important advantage of non-linear approaches is that heating rates can be optimized over particular temperature ranges to improve analytical precision and decrease overall experimental run time. For example, heating schedules that are linear in 1/T focus proportionally more analytical time on the early portion of gas release, where He losses are small and analytical precision is low (Fig. 1). Although non-linear heating ramps may be advantageous in some circumstances, the ability to employ them effectively may be limited by the capabilities of the instrumentation used for the experiments (e.g., commercial programmable temperature controllers are generally limited to heating schedules that follow linear temperature ramps).

At the start of our continuous heating experiments samples were brought rapidly to an initial temperature of ~200°C, either by dropping them into the furnace crucible held at that temperature or by ramping the laser power. The mass spectrometer was then isolated from its associated ion pump but kept open to the extraction line for the entire duration of the experiment. The sample temperature was then increased linearly to 1000-1150°C during typical experiment durations of 30-75 minutes. The laser experiments were conducted using a constant ramp rate of 30°C/min, and the sample temperature was measured directly using the embedded thermocouple. At this heating rate the measured sample temperature tracked the programmed ramp temperature to better than 1°C across the entire experimental temperature range. This degree of control is comparable to or better than that achieved by the projector bulb heating apparatus described by Farley et al. (1999), with the added advantage that the laser system is not subject to the ~750°C maximum temperature limit of the projector bulb apparatus.

Slower ramp rates of 15-20°C/min were used for the low-temperature part of the release during furnace runs to minimize thermal lag associated with heating the relatively large mass of the sample crucible and to provide additional time for gettering the higher hydrogen load produced by the furnace. For furnace runs, the initiation of the temperature ramp was synchronized with the start of data collection, and sample temperature was inferred from the programmed ramp rate. At ramp rates of 20°C/min or less the temperature at the base of the sample crucible tracked the programmed ramp temperature closely, generally deviating by no more than ~5°C. However,

kinetic parameters calculated from Durango apatite He loss data for furnace runs suggest that a significant temperature gradient of up to 75°C existed between the thermocouple at the base of the crucible and the sample during the furnace CRH runs (see section 3). To better constrain the sample temperature, ramped heating calibration experiments were conducted at various heating rates using an additional W-Re thermocouple located at the sample position inside the Mo liner. Temperature offsets between the interior and exterior (controlling) thermocouples ranged from ~30 to 50°C for a ramp rate of 20°C/min. The results of these calibration runs were used to correct the sample temperatures inferred from the external thermocouple measurements during the CRH experiments. The corrections provide a more realistic estimate of the actual sample temperature experienced by samples during furnace CRH experiments, but comparison of corrected He release curves and kinetic data for Durango apatite run using furnace and laser heating show that discrepancies of up to ~30°C still remain at low extraction temperatures. We suspect that poor conductive heat transfer between the crucible, crucible liner, and sample packets caused by limited contact area and irregular stacking of packets may have been responsible for some or all of the observed temperature offset.

Gas evolved from the samples was purified continuously in the extraction line by SAES GP50 and HI/20-10/650C getters operated at room temperature. Measurement of the  $^4$ He released during the experiments was performed continuously over the course of the CRH experiments. The quadrupole mass spectrometer was operated at 200  $\mu$ A total emission in order to minimize the rate of  $^4$ He consumption, and all measurements were made with a Channeltron electron multiplier operated in the analog mode. Between 90 and 225 measurements were made over the duration of each run. Integration times of 10-20 seconds were used for the  $^4$ He measurements, and beams at m/z 1, 2, and 3 were also measured during each cycle using a 0.5 second integration time to monitor hydrogen, the most significant contributor to total pressure in the mass spectrometer during the CRH experiments. We determined  $^4$ He abundances manometrically by comparison of peak heights with those obtained from a mixed  $^4$ He/ $^3$ He standard containing  $\sim$ 0.22 pmoles  $^4$ He that was analyzed between continuous heating runs. We have also recently begun to check instrument sensitivity independently by introducing an aliquot of this standard into the sample gas at the end of CRH runs and calculating the final total  $^4$ He abundance using the method of standard additions.

For CRH data, calculation of kinetic parameters followed the standard methodology used for traditional step-heating experiments: incremental He measurements were treated mathematically as arising from square-pulse heating steps after subtraction of the signal from the previous measurement. Assignment of temperature values to heating intervals was complicated by the fact that sample temperatures increased linearly through a range of up to 10°C during each ~20 second measurement interval. Instead of using the average value as our estimate of the effective temperature for each interval, we typically used the temperature attained at ~60% of the interval duration, in order to account for enhanced release at higher temperatures. We estimate the uncertainty in the assigned effective temperatures to be less than 2°C. Kinetic parameters reported in section 3 were calculated using spherical diffusion geometry (Carslaw and Jaeger, 1959; see also Fechtig and Kalbitzer, 1966).

Data from CRH experiments can be depicted in two forms (e.g., Figures 1, 4, and 6). Cumulative-loss (f) curves show the accumulated fractional He loss over the course of an experiment normalized to complete loss (= 1.0), consistent with the general convention employed for step-heating experiments. Cumulative losses are plotted as a function of experimental temperatures obtained by linking the sample heating and mass-spectrometer time series, as discussed above. Cumulative-loss data can be numerically differentiated to obtain incremental-loss curves, which show He released during each repetitive measurement cycle (df) or He release normalized to temperature interval (df/dT). Because measured beams are small at the beginning of an experiment and change little at the beginning and the end, the incrementalrelease data can be noisy, so we generally plot a three-point running average to reduce this noise and emphasize the general form of the curves. It is important to keep in mind that the overall forms of both cumulative- and incremental-loss curves and the positions of the curves along the temperature axis will depend upon the temperature ramp rate employed during the experiments (Fig. 1). For incremental-loss plots depicting He loss per step (df plots), areas beneath df curves are not conserved as ramp rates are varied, which complicates comparison of results obtained from experiments run at different ramp rates. For this reason, it is advantageous to normalize incremental-loss data to temperature interval (i.e., express losses as df/dT) if ramp rates will be varied during a CRH study. Even so, because of the overall non-linear Arrhenius behavior shown by apatites for He diffusion (e.g., Farley, 2000; Shuster et al., 2006), it is not possible to easily compare data collected using different heating protocols.

#### 3. Results and discussion

To date we have performed CRH experiments on ~200 apatite samples that span a wide range of ages and geologic settings (McDannell et al., in review). Representative results for the Durango apatite age standard and three additional samples are presented in this section. Analytical data for the CRH runs are provided in supplementary table A.1.

### 3.1 Continuous heating experiments on Durango apatite

Cumulative- and incremental-loss curves for four shards of the Durango apatite standard analyzed using the CRH method are shown in Fig. 4. The loss curves for the two furnace runs (DUR-1 and DUR-2) are shifted slightly toward higher temperatures relative to those for the laser experiments, possibly reflecting differences in the effective grain sizes or grain shapes of the samples or the presence of residual temperature offset and lag in sample heating that was not fully corrected for using the dual thermocouple calibration described in section 2. Despite these small differences, the overall forms of both the cumulative- and incremental-loss curves conform well to those predicted by volume diffusion models using empirically determined Durango kinetic parameters (Fig. 1).

Low-temperature results for the two laser runs (DUR-3 and DUR-4) exhibit linear Arrhenius behavior (Fig. 5). Although there is significant scatter in the first few measurements for each experiment, these measurements represent very small He fractions with high analytical uncertainties. Excluding these early points, regression of the low-temperature measurements (T<350°C) yields activation energies ( $E_a$ ) of 135 and 139 kJ/mole for DUR-3 and DUR-4, respectively and a  $ln(D_0/a^2)$  value of 12.6 s<sup>-1</sup> for both samples. The corresponding He closure temperatures ( $T_c$ ) are 69°C for DUR-3 and 78°C for DUR-4 (calculated assuming a cooling rate of 10°C/my). These results agree well with those obtained from detailed step-heating experiments by Farley (2000), who quoted average values of ~138 kJ/mole for  $E_a$  and 0.50 m<sup>2</sup>-s<sup>-1</sup> for  $D_0$ . Assuming a grain size of 200  $\mu$ m, these parameters correspond to a value for  $ln(D_0/a^2)$  of 13.1 and a closure temperature of ~74°C.

A decrease in the slope of both laser-heating CRH Arrhenius curves is evident beginning at temperatures of ~350°C, and the slopes shallow significantly above 425-450°C. Similar changes

in kinetic behavior have been documented in other laboratory outgassing studies of Durango apatite, and the change has been proposed to be associated with annealing of alpha and fission tracks that serve as traps for He (Farley, 2000; Schuster et al., 2006; Gautheron et al., 2009; Shuster and Farley, 2009). Alpha tracks comprise the bulk of the dominant radiation damage in natural apatites, but Shuster et al. (2009) showed that the kinetics of alpha track annealing closely follow those for fission tracks. Although it is not clear from a mechanistic perspective how annealing of traps would lead to lower values of diffusivity at moderate to high temperatures, we note that the transition to lower activation energies observed during our CRH experiments coincides broadly with the intermediate and final stages of radiation damage annealing in Durango apatite: for the laboratory heating schedule used during our laser CRH runs, the fission-track annealing models of Laslett et al. (1987) and Ketcham et al. (2007) predict ~50% track length reduction in Durango apatite by 310-330°C, and >98% reduction by 400-450°C.

The onset of the transition in kinetic behavior in the published step-heating studies (e.g., ~265°C, Farley, 2000; ~325°C, Shuster et al., 2006) occurred at lower temperatures than we observed during our CRH runs, but this result is expected if the process controlling the transition is thermally activated, since the step-heating experiments employed much longer heating durations. The dependence of the transition temperature on the laboratory heating schedule has interesting consequences for CRH experiments. The step-heating studies of Farley (2000) and Shuster et al. (2006) relied on heating times of many hours or days to achieve measureable He losses at temperatures as low as ~120°C, presumably with the aim of extending the linear portions of the Arrhenius curves toward lower temperatures to provide a more robust assessment of the kinetic parameters governing He loss. In fact, these step-heating experiments were initiated at temperatures ~100°C lower than those at which we could begin to reliably measure losses during our CRH runs. However, long heating steps lead to early annealing of radiation damage and a transition in diffusion behavior at relatively low temperatures. For example, for a series of 1 hr. long heating steps beginning at 120°C and incrementing by 5°C, the aforementioned fissiontrack annealing models predict 50% track length reduction by ~240°C, about 80° lower than the corresponding temperature for our laser CRH runs. The rapid heating schedule employed in our CRH experiments precludes measurements at very low temperatures (< 200°C) but delays

annealing and pushes linear behavior toward higher temperatures, where He diffusivities are high and short heating increments result in large losses that are easily measured. This tradeoff maintains linear behavior over a reasonably wide temperature range during CRH experiments and allows the linear portion of the Arrhenius curve to be characterized very quickly (< 10 min. in our experiments).

Arrhenius plots for two furnace CRH experiments using Durango apatite are also shown in Fig. 5. The curves follow the general trend of the laser results, but with some additional artifacts. Like the furnace cumulative- and incremental-loss curves, the Arrhenius results are offset slightly toward higher temperatures throughout much of the He release. The offset decreases toward higher temperatures, probably reflecting a change in the relative proportions of radiative and conductive heat transfer in the furnace and a corresponding improvement in our temperature calibrations as the experiments progress. Additionally, the slopes of the Arrhenius curves for the furnace runs are anomalously steep below 300°C, particularly in the case of DUR-2. Since these experiments were started with the furnace at a steady temperature of 200°C, the initial steep slopes probably reflect our inability to fully correct for thermal lag associated with the start of the heating ramp, which diminished or disappeared once the temperature gradients within the crucible stabilized. It is evident from these results that CRH experiments using large doublevacuum resistance furnaces do not provide the critical temperature control needed to characterize kinetic parameters accurately. However, we reiterate that the overall forms of the cumulativeand incremental-loss curves obtained from furnace CRH experiments are similar to those obtained from laser-heating experiments, and as we show below, furnace CRH experiments are quite capable of distinguishing between different modes of He release behavior in natural apatite samples.

### 3.2 Contrasting modes of He loss in other natural apatites

Our CRH experiments document a wide range of behaviors, with some samples showing simple He release curves like those obtained from Durango apatite, and others more complex behavior characterized by cumulative loss curves with multiple inflection points and incremental loss curves exhibiting two or more peaks and/or sharp spikes in He release. Many apatites that show complex behavior during CRH experiments contain a significant He component that is released at anomalously high experimental temperatures, and this behavior appears to be correlated with

highly dispersed and often unrealistically old conventional U-Th/He apatite ages. A full summary of the observed styles of He release that we have observed is beyond the scope of this discussion but will be addressed in a companion paper (McDannell et al., in review). However, we present data for four apatite grains from three representative samples that illustrate the ability of the CRH method to discriminate between samples that show the simple mode of He outgassing predicted by volume diffusion theory and those that exhibit anomalous outgassing behavior.

Helium loss curves for two optically clear, inclusion-free apatite crystals from Mongolian granite 14MN07 are shown in Fig. 6. The CRH runs were performed using furnace heating with a  $20^{\circ}$ C/min ramp rate, and yielded U-Th/He ages of 105 and 94 Ma. The  $\sim$ 10% disparity in these ages can be reasonably explained by analytical uncertainties and differences in the size and eU of the two grains. The CRH results are nearly identical with regard to He evolution. Both grains yield smooth sigmoidal cumulative loss curves and slightly asymmetrical incremental loss curves showing peak release at  $\sim$ 625°C, similar to what was observed in the Durango apatite CRH experiments. More than 99.9% of the total He in these samples was released by 900°C.

Markedly different CRH results were obtained from Tibetan samples NB07 and NB54, which were identified as "bad actor" samples during the course of a conventional U-Th/He dating study (Zeitler et al., 2014). Three single-grain analyses of NB07 apatite yielded U-Th/He ages of 11, 14, and 25 Ma, while nearby samples have ages of ~7-8 Ma and show low age dispersion. Replicate analyses of NB54 apatite yielded single-grain ages of 14, 55, and 204 Ma, yet this sample has an expected age of ~2-7 Ma based upon results from better-behaved samples nearby. The CRH cumulative loss curves for these samples have multiple inflection points and are displaced significantly toward high temperatures relative to those for 14MN07 and Durango apatite (Fig. 6). At low to moderate temperatures, the incremental loss curve for NB54-1 shows a peak centered at ~650°C that is probably correlative with the single volume diffusion peaks observed for 14MN07 and Durango apatite. However, the NB54-1 peak appears lower in amplitude due to the broad, bimodal nature of the release and the requirement that total cumulative losses equal 1 in all these plots. Over the same temperature interval, the NB07-1 incremental loss curve contains a very broad and diffuse peak centered at ~600°C that is punctuated by several sharp spikes in He release between 500 and 600°C. At higher

temperatures, the incremental loss curves for both of these samples contain prominent peaks centered well above 900°C, the temperature marking complete outgassing of most well-behaved apatites. The component released above 900°C accounts for  $\sim$ 40% of the total He released from NB07-1 and  $\sim$ 60% of that from NB54-1.

Both the anomalous He release at temperatures >900°C and the transient release at lower temperatures observed during our "bad actor" CRH experiments represent behavior that cannot be readily explained by volume-diffusion theory, even when modified to take into account the effects of radiation damage on He diffusion (e.g., Shuster et al., 2006; Flowers et al., 2009). We propose that trapping of He in fluid inclusions or other microvoids is responsible for both of these effects (see Zeitler et al., 2017 for a more detailed discussion). The source of this trapped He is uncertain. It may be an excess component derived from external sources that becomes trapped in fluid inclusions or other voids during grain growth or deformation (e.g., Stockli et al., 2000). Alternatively, in the case of slowly cooled samples that reside for extended periods at elevated temperatures in the He partial retention zone, autogenic radiogenic He that would normally be expected to diffuse partially or completely out of grains could become trapped in microvoids, resulting in a form of self-contamination. We suggest that the He released as transient spikes at low to moderate laboratory temperatures is hosted in microvoids that are breached mechanically (i.e., by decrepitation or related processes) during laboratory heating, while the high-temperature release occurs when diffusivity increases sufficiently to allow He trapped in intact microvoids to reenter the apatite crystal lattice.

Regardless of its source and siting, our experiments suggest that all or part of this He represents a component not normally found in pristine samples that presumably lack microvoids or other microstructural traps, and its presence skews U-Th/He results toward older ages and leads to increased age dispersion. The CRH method is an effective and relatively simply way to detect such anomalously sited He in apatite and to assess the extent to which it may have polluted a sample. Paradoxically, one of the main concerns during single-step heating experiments typically employed for conventional U-Th/He dating is to insure that the sample is heated sufficiently to release *all* of the He it contains. This approach can lead to incorrect results for those samples that contain anomalously sited He. A common U-Th/He experimental protocol is to subject samples to relatively high temperatures for several minutes or longer, then follow this "analysis" step

with a second "re-extraction" step, typically at a higher temperature, to confirm total He loss and in some cases to assess whether there has been any anomalous He release (House et al., 2000; Farley, 2002). Temperatures for the main analysis step reported in recent published papers on apatite U-Th/He dating are commonly in the 900-950°C range, but some laboratories report using temperatures of 1050°C or higher (e.g., Gautheron et al., 2009; Grasemann et al., 2012). Other published studies do not report laboratory extraction temperatures at all, possibly because instrumentation for precise sample temperature determination was not available. In such situations the temperature is often assessed by visual inspection of the color of the black-body radiation emitted by the incandescent sample (e.g., Foeken et al., 2006; Ault et al., 2016), or controlled by limiting the laser power to a predetermined level that may be based upon an earlier calibration (e.g., Schildgen et al., 2009; McDermott et al., 2013). Both of these methods may be subject to considerable uncertainty. Regardless of the experimental protocol used, in cases where the temperature of the initial heating step is set sufficiently high (either knowingly or unwittingly), there is a significant likelihood that any anomalously sited He present in the sample will be released along with "normal" lattice-sited He.

The results from CRH experiments can be used to define heating schedules for conventional single-step heating experiments that ensure complete He extraction from well-behaved samples while still allowing a subsequent re-extraction step to identify the presence of anomalously sited He. Evaluation of our CRH results shows that heating to 900°C with ramp rates of 20-30°C/min results in near-complete He loss (>99.5%, integrated  $Dt/a^2 \sim 0.5$ ) for well-behaved samples with simple He release patterns. Transforming this result into an equivalent single square heating pulse is not straightforward, since the kinetics of He loss during a rapid high-temperature heating pulse are not well constrained. However, published models for fission-track annealing (Laslett et al., 1987; Ketcham et al., 2007) suggest that radiation damage should anneal completely in a few seconds at the extraction temperatures typically employed in apatite U-Th/He experiments. If so, the rate of He outgassing during single-step extraction experiments should be governed almost entirely by kinetic parameters appropriate for damage-free apatites. Assuming published diffusion constants for fully annealed, damage-free Durango apatite ( $E_a = 122.3 \text{ kJ/mol}$ ,  $\ln(D_0/a^2)$ = 9.733; Flowers et al., 2009), heating at 900°C for ~10 s should be sufficient to insure >99.9% He release from Durango apatite during single-step experiments. In practice, heating times should be significantly longer than this to account for variations in high-temperature He

retentivity in natural apatites, thermal lag during heating, temperature measurement errors, and other sources of experimental uncertainty. We tentatively suggest that heating times on the order of 2-3 minutes at 900°C should provide a sufficient safety margin to insure complete release of lattice-sited He in most natural apatites. Helium released subsequently during a re-extraction step at a higher temperature would then likely represent a trapped component derived from microvoids or other non-lattice sites. In summary, if the parameters of a single heating step are controlled carefully, a subsequent re-extraction step provides a useful test for the presence of trapped He released at high experimental temperatures. However, it is important to note that re-extraction steps cannot be used to identify samples that have anomalously sited He released as spikes at low to moderate temperatures (e.g., our sample NB07-1).

#### 4. Conclusions

The CRH method represents a promising new tool for characterizing the distribution and release of He in apatite during U-Th/He dating experiments. The method carries with it several significant analytical challenges, but in most cases they can be surmounted effectively by modest modifications to existing experimental hardware and protocols. In addition to careful temperature control during sample heating, particular attention must be paid to minimizing the buildup of hydrogen and other contaminating gas species in the mass spectrometer, achieving good gas conductance within the extraction system, and insuring good measurement linearity over a wide range of gas pressures. Continuous heating experiments can be conducted in little more time than is required to perform the conventional two-step (extraction/re-extraction) heating experiments commonly employed for apatite U-Th/He dating.

In addition to providing a measure of total <sup>4</sup>He for age calculation, the CRH method offers several important advantages over conventional analytical approaches. The continuous record of He evolution over a wide range of temperatures obtained from these experiments allows He diffusion kinetics to be assessed quantitatively during routine apatite U-Th/He dating experiments, as demonstrated by the close agreement between kinetic parameters obtained from our CRH experiments on the Durango apatite age standard and those derived from lengthy conventional step-heating studies. More importantly, CRH experiments reveal important information about the siting of He atoms in apatite and help to identify He components present in some samples whose behavior does not obey volume diffusion laws (modified as necessary for

the effects of radiation damage). In addition to its potential as a powerful screening tool for apatite samples, we suggest that the CRH method can provide insights into the physical causes of high age dispersion in U-Th/He data sets that cannot be gleaned from age data alone. Effort is underway in our laboratory to use the results of CRH experiments to more fully characterize the range of He release patterns observed in natural apatites, to understand their origins, and to develop methods for extracting useful age information from samples affected by anomalously sited He (McDannell et al., in review).

### Acknowledgments

We thank Marty Grove and Kendra Murray for insightful reviews, and Klaus Mezger for editorial handling of the manuscript. Portions of this work were supported by NSF grant EAR-1049944 from the Petrology and Geochemistry program.

#### References

- Carslaw, H.S., and Jaeger, J.C., 1959, *Conduction of Heat in Solids*, 2nd ed. Clarendon Press, Oxford.
- Cowan, M.C., Allison, W., and Batey, J.H., 1994, Nonlinearities in sensitivity of quadrupole partial pressure analyzers operating at higher gas pressures. J. Vac. Sci. Technol. A, v. 12, p. 228-234, doi:10.1116/1.578888.
- Farley, K.A., 2000, Helium diffusion from apatite: General behavior as illustrated by Durango fluorapatite. Journal of Geophysical Research, v. 105, p. 903–2914, doi:10.1029/1999JB900348.
- Farley, K. A., 2002, (U-Th)/He dating: Techniques, calibrations, and applications. Reviews in Mineralogy and Geochemistry, v. 47, p. 819-844, doi:10.2138/rmg.2002.47.18.
- Farley, K.A., Reiners, P.W., and Nenow, V., 1999, An apparatus for high-precision helium diffusion measurements from minerals. Anal. Chem., v. 71 p. 2059-2061, doi:10.1021/ac9813078.
- Farley, K.A., Shuster, D.L., and Ketcham, R.A., 2011, U and Th zonation in apatite observed by laser ablation ICPMS, and implications for the (U–Th)/He system. Geochimica et Cosmochimica Acta, v. 75, p. 4515-4530, doi:10.1016/j.gca.2011.05.020.

- Fechtig H., and Kalbitzer S., 1966, The diffusion of argon in potassium-bearing solids. In *Potassium Argon Dating* (eds. O.A. Schaeffer and J. Zahringer). Springer-Verlag, New York, pp. 68–106.
- Fitzgerald, P.G., Baldwin, S.L., Webb, L.E., and O'Sullivan, P.B., 2006, Interpretation of (U-Th)/He single grain ages from slowly cooled crustal terranes: A case study from the Transantarctic Mountains of southern Victoria Land. Chemical Geology, v. 225, p. 91-120, doi:10.1016/j.chemgeo.2005.09.001.
- Flowers, R.M., and Kelley, S.A., 2011, Interpreting data dispersion and "inverted" dates in apatite (U-Th)/He and fission-track datasets: An example from the US midcontinent.

  Geochimica et Cosmochimica Acta, v. 75, p. 5169-5186, doi:10.1016/j.gca.2011.06.016.
- Flowers, R.M., Ketcham, R.A., Shuster, D.L., and Farley, K.A., 2009, Apatite (U-Th)/He thermochronometry using a radiation damage accumulation and annealing model.

  Geochimica et Cosmochimica Acta, v. 73, p. 2347-2365, doi:10.1016/j.gca.2009.01.015.
- Gautheron, C., Tasan-Got, L., Barbarand, J., and Pagel, M., 2009, Effect of alpha-damage annealing on apatite (U-Th)/He thermochronology. Chemical Geology, v. 266, p. 157-170, doi:10.1016/j.chemgeo.2009.06.001.
- Gautheron, C., Tasan-Got, L., Ketcham, R.A., and Dobson, K.J., 2012, Accounting for long alpha-particle stopping distances in (U-Th-Sm)/He geochronology: 3D modeling of diffusion, zoning, implantation, and abrasion. Geochimica et Cosmochimica Acta, v. 96, p. 44-56, doi:10.1016/j.gca.2012.08.016.
- Gerin, C., Gautheron, C., Oliviero, E., Bachelet, C., Djimbi, M.D., Seydoux-Guillaume, A.M., Tassan-Got, L., Sarda, P., Roques, J., and Garrido, F., 2017, Influence of vacancy damage on He diffusion in apatite, investigated at atomic to mineralogical scales. Geochimica et Cosmochimica Acta, v. 197, p. 87-103, doi:10.1016/j.gca.2016.10.018.
- Gerling, E.K., Levskii, L.K., and Morozova, I.M., 1963, On the diffusion of radiogenic argon from minerals. Geochemistry, v. 6, p. 551-555.
- Grasemann, B., Schneider, D.A., Stöckli, D.F., and Iglesder, C., 2012, Miocene bivergent crustal extension in the Aegean: Evidence from the western Cyclades (Greece). Lithosphere, v. 4, p. 23-39, doi:10.1130/L164.1.

- House, M.A., Farley, K.A., and Stockli, D., 2000, Helium chronometry of apatite and titanite using Nd-YAG laser heating. Earth and Planetary Science Letters, v. 183, p. 365-368, doi:10.1016/S0012-821X(00)00286-7.
- Ketcham, R.A., Carter, A., Donelick, R.A., Barbarand, J., and Hurford, A.J., 2007, Improved modeling of fission-track annealing in apatite. Am. Min., v. 92, p. 799-810, doi:10.2138/am.2007.2281.
- Levskii, L.K., 1963, Diffusion of helium from stony meteorites. Geochemistry, v. 6, p. 556-561.
- Lieszkovszky, L., Filippelli, A.R., and Tilford, C.R., 1990, Metrological characteristics of a group of quadrupole partial pressure analyzers. J. Vac. Sci. Technol. A, v. 8, p. 3838-3854, doi:10.1116/1.576458.
- McDannell, K.T., Zeitler, P.K., Janes, D.G., Idleman, B.D., and Fayon, A.K., Screening apatites for (U-Th)/He thermochronometry via continuous ramped heating: Helium age components and implications for age dispersion. Geochim. Cosmochim. Acta (in review).
- McDermott, J.A., Whipple, K.X., Hodges, K.V., and van Soest, M.C., 2013, Evidence for Plio-Pleistocene north-south extension at the southern margin of the Tibetan Plateau, Nyalam region. Tectonics, v. 32, p. 317–333, doi:10.1002/tect.20018.
- McDowell, F., McIntosh, W. and Farley, K., 2005, A precise <sup>40</sup>Ar-<sup>39</sup>Ar reference age for the Durango apatite (U-Th)/He and fission-track dating standard. Chemical Geology, v. 214, p. 249–263, doi:10.1016/j.chemgeo.2004.10.002.
- McKeon, R.E., Zeitler, P.K., Pazzaglia, F.J., Idleman, B.D., and Enkelmann, E., 2014, Decay of an old orogen: Inferences about Appalachian landscape evolution from low-temperature thermochronology. Geological Society of America Bulletin, v. 126, p. 31-46, doi:10.1130/B30808.1.
- Murray, K.E., Orme, D.A., and Reiners, P.W., 2014, Effects of U-Th-rich grain boundary phases on apatite helium ages. Chemical Geology, v. 390, p. 135-151, doi:10.1016/j.chemgeo.2014.09.023.
- Schildgen, T.F., Ehlers, T.A., Whipp Jr., D.M., van Soest, M.C., Whipple, K.X., and Hodges, K.V., 2009, Quantifying canyon incision and Andean Plateau surface uplift, southwest Peru: A thermochronometer and numerical modeling approach. J. Geophys. Res., v. 114, F04014, doi:10.1029/2009JF001305.

- Shuster, D.L., and Farley, K.A., 2009, The influence of artificial radiation damage and thermal annealing on helium diffusion kinetics in apatite. Geochim. Cosmochim. Acta, v. 73, p. 183-196, doi:10.1016/j.gca.2008.10.013.
- Shuster, D.L., Flowers, R.M., and Farley, K.A., 2006, The influence of natural radiation damage on helium diffusion kinetics in apatite. Earth and Planetary Science Letters, v. 249, p. 148-161, doi:10.1016/j.epsl.2006.07.028.
- Spiegel, C., Kohn, B.P., Belton, D., and Gleadow, A. J., 2009, Apatite (U–Th–Sm)/He thermochronology of rapidly cooled samples: The effect of He implantation. Earth and Planetary Science Letters, v. 285, p. 105-144, doi:10.1016/j.epsl.2009.05.045.
- Vermeesch, P., Seward, D., Latkoczy, C., Wipf, M., Günther, D., and Baur, H., 2007, α-Emitting mineral inclusions in apatite, their effect on (U–Th)/He ages, and how to reduce it. Geochimica et Cosmochimica Acta, v. 71, p. 1737-1746, doi:10.1016/j.gca.2006.09.020.
- Warnock, A.C., Zeitler, P.K. Wolf, R.A., and Bergman, S.C., 1997, An evaluation of low-temperature apatite U-Th/He thermochrometry. Geochim. Cosmochim. Acta, v. 61, p. 5371-5377, doi:10.1016/S0016-7037(97)00302-5.
- Willett, C.D., Fox, M., and Shuster, D.L., 2017, A helium-based model for the effects of radiation damage annealing on helium diffusion kinetics in apatite. Earth and Planetary Science Letters, v. 477, p. 195-204, doi:10.1016/j.epsl.2017.07.047.
- Wolf, R.A., Farley, K.A., and Silver, L.T., 1996, Helium diffusion and low temperature thermochronometry of apatite. Geochim. Cosmochim. Acta, v. 60, p. 4231-4240, doi:10.1016/S0016-7037(96)00192-5.
- Young, E., Myers, A., Munson, E., and Conklin, N., 1969, Mineralogy and geochemistry of fluorapatite from Cerro de Mercado, Durango, Mexico. U.S. Geological Survey Professional Paper 650-D, p. D84–D93.
- Zeitler, P.K., Herczeg, A., McDougall, I., and Honda, M., 1987, U-Th-He dating of Durango fluorapatite: a potential thermochronometer. Geochimica et Cosmochimica Acta, v. 51, p. 2865-2868, doi:10.1016/0016-7037(87)90164-5.
- Zeitler, P.K., Enkelmann, E., Thomas, J.B., Watson, E.B., Ancuta, L.D., and Idleman, B.D., 2017, Solubility and trapping of helium in apatite. Geochimica et Cosmochimica Acta, v. 209, p. 1-8, doi:10.1016/j.gca.2017.03.041.

Zeitler, P.K., Meltzer, A.S., Brown, L., Kidd, W.S.F., Lim, C., and Enkelmann, E., 2014, Tectonics and topographic evolution of Namche Barwa and the easternmost Lhasa block, Tibet., *in* Nie, J., Horton, B.K., and Hoke, G.D., eds., Toward an Improved Understanding of Uplift Mechanisms and the Elevation History of the Tibetan Plateau: Geological Society of America Special Paper 507, p. 23–58, doi:10.1130/2014.2507(02).

### **Figure Captions**

**Figure 1.** Predicted cumulative (A) and incremental-loss (B) curves for  $^4$ He release from Durango apatite during CRH analyses. Plots assume spherical diffusion geometry,  $E_a = 138$  kJ/mole,  $D_0 = 5 \times 10^{-3}$  m²/s, effective diffusion radius = 100  $\mu$ m, measurement interval = 20 s, and heating over the interval 200-800°C. Results are shown for four linear heating rates (solid and dashed lines) and one heating schedule where temperature is linear in 1/T (open circles). The incremental-loss curves (B) represent the first derivative of the cumulative-loss data (A), expressed as fraction of total He loss per °C (df/dT). Note that compared with these model results, experimentally derived curves will be offset slightly toward higher temperatures due to the change in kinetics displayed by most apatite samples at temperatures of about 300°C (Farley, 2000).

**Figure 2.** Contributions from system <sup>4</sup>He blank and <sup>4</sup>He consumption during CRH analysis of Durango apatite sample DUR-4 (see section 3 for analytical results). The blank curve shows the <sup>4</sup>He blank component as a percentage of the cumulative <sup>4</sup>He released at the time of each measurement. The consumption curve represents a maximum estimate determined using the consumption rate appropriate for the <sup>4</sup>He partial pressure experienced at the end of the CRH experiment.

**Figure 3.** Pressure linearity of the quadrupole mass spectrometer used for the CRH experiments. With the exception of the smallest measurement, analytical uncertainties  $(2\sigma)$  are smaller than the symbols. Regression of the original data (before log-log transformation) yields a y-intercept indistinguishable from zero and  $R^2 > 0.999$ .

**Figure 4.** Cumulative (A) and incremental (B)  $^4$ He loss curves for single fragments of Durango apatite analyzed using the CRH method. The heating rates used for furnace runs DUR-1 and DUR-2 were 20 and 30°C/min, respectively. Samples DUR-3 and DUR-4 were analyzed using laser heating at 30°C/min. Results were smoothed using a 3-point running average to reduce noise and emphasize the overall form of the curves. The measurement interval for furnace runs was  $\sim$ 22 s and for laser runs  $\sim$ 12 s.

**Figure 5.** Arrhenius plots for laser and furnace CRH experiments using Durango apatite. (A) Overall results for furnace and laser-heated runs. (B) Detail of low-temperature interval for laser runs DUR-3 and DUR-4 showing data used to calculate diffusion parameters. Solid circles/red line: data points and associated regression line for DUR-3 (points 5-28,  $R^2$ =0.996). Solid diamonds/blue line: data points and associated regression line for DUR-4 (points 6-29,  $R^2$ =0.997). Open symbols denote data points not included in the regressions. Analytical uncertainties in  $ln(D/a^2)$  are on the order of symbol size. Dashed line: low-temperature results for Durango apatite from Farley (2000).

**Figure 6.** Cumulative (A) and incremental (B) <sup>4</sup>He loss curves for apatite from Mongolian granite 14MN07 and Tibetan gneisses NB07 and NB54 analyzed using the CRH method. Results were smoothed using a 3-point running average to reduce noise and emphasize the overall form of the curves. The heating rates for the two 14MN07 runs were 20°C/min. NB07 and NB54 were heated at 15°C/min to 950°C, and 20°C/min above 950°C. In addition to the ramped heating, NB07 was held isothermally at 1150°C for ~4.5 minutes at the end of the experiment. The curves for NB07-1 and NB54-1 are based upon observed losses but are approximations, since neither sample was outgassed completely despite being heated to 1150°C, and their total <sup>4</sup>He contents are not known. The measurement interval for all runs was ~22 s.

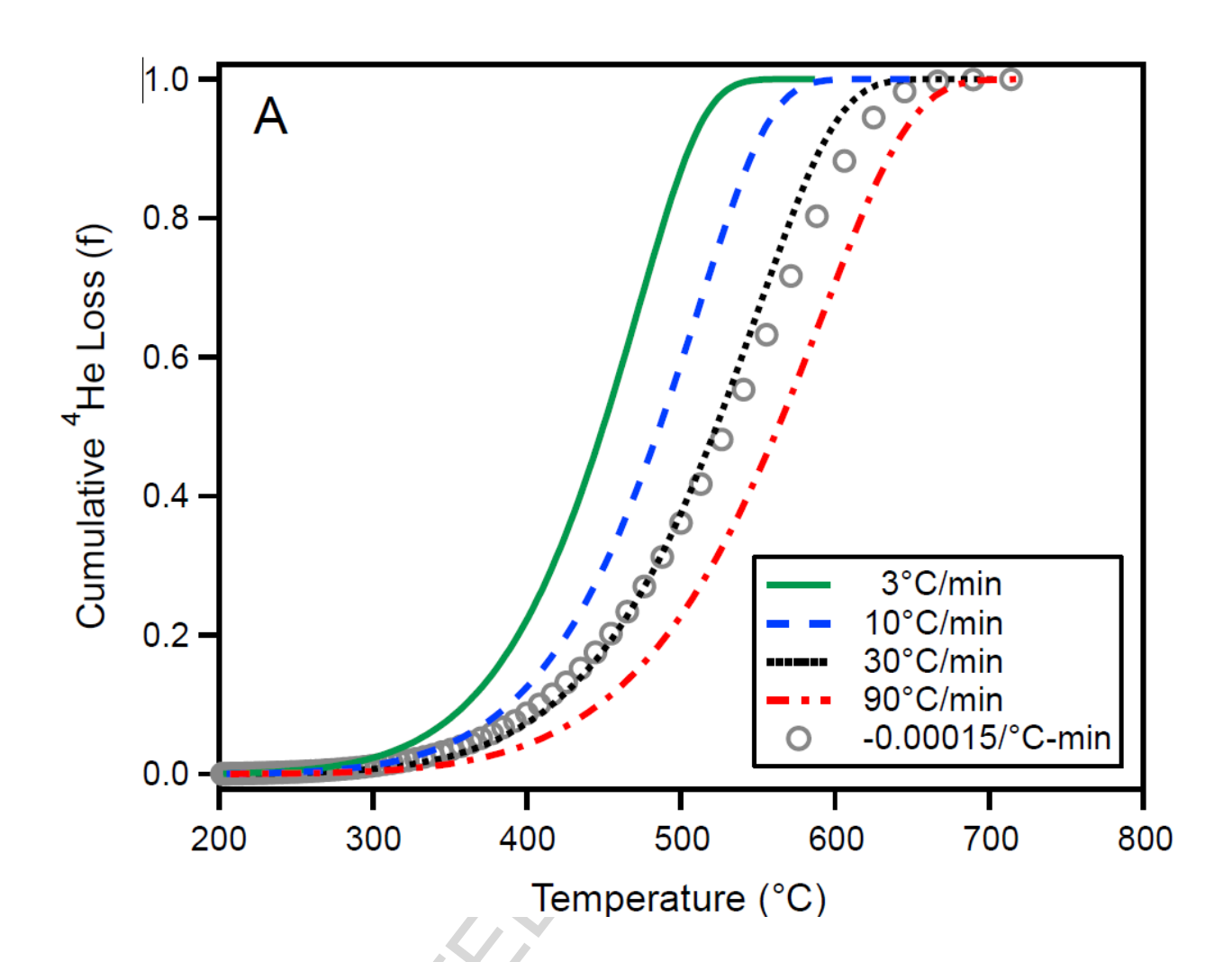


Fig. 1A

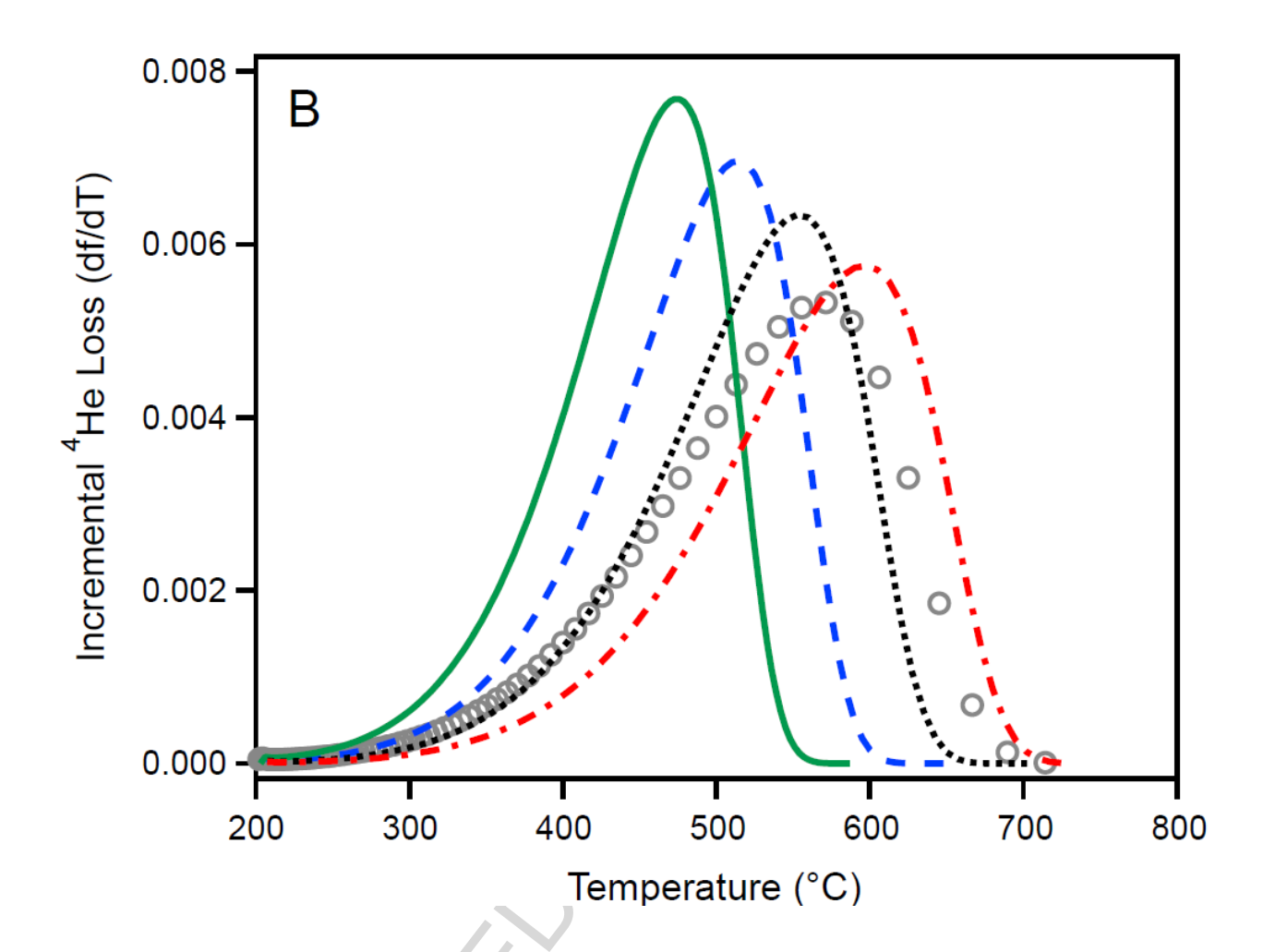


Fig. 1B

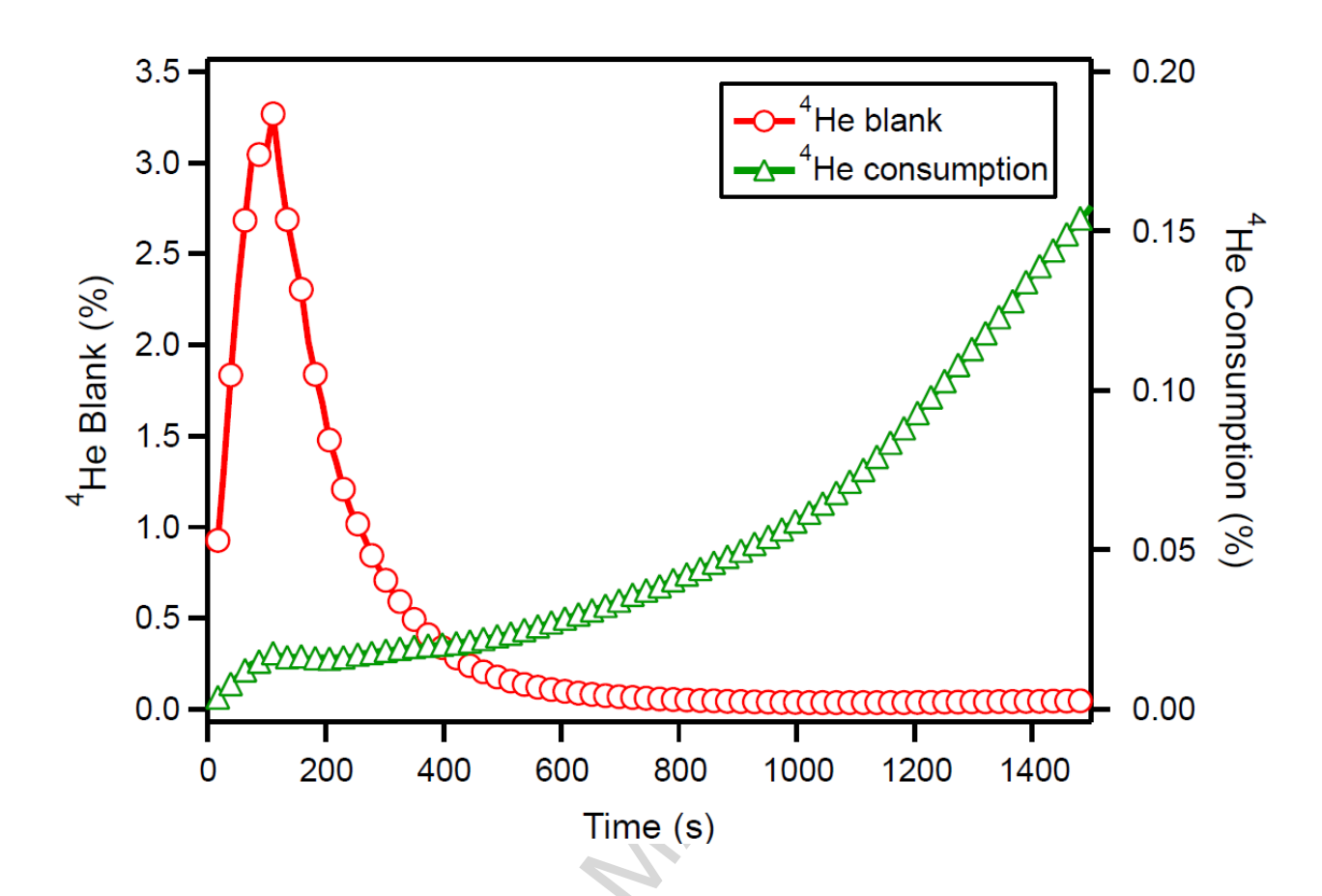


Fig. 2

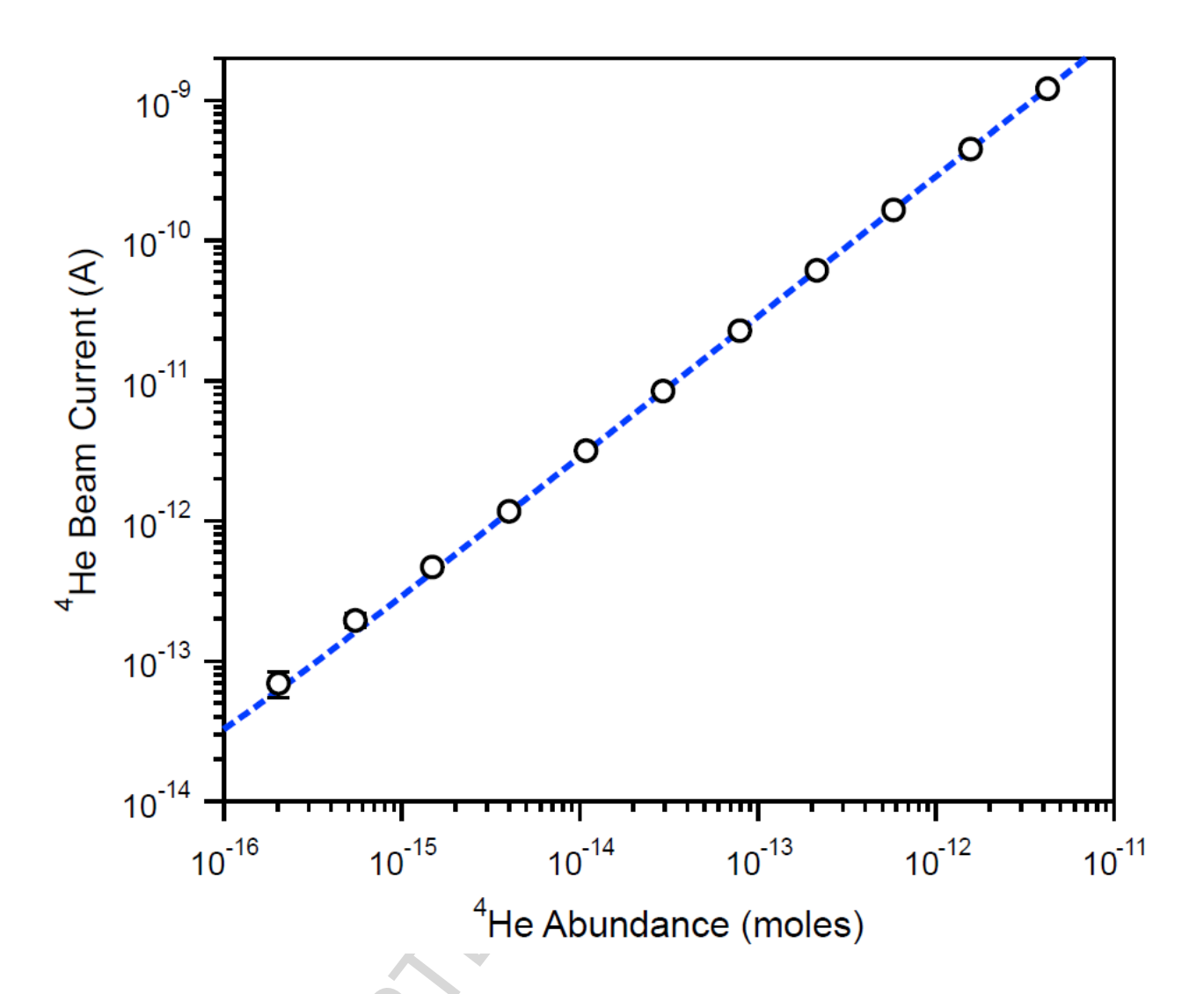


Fig. 3

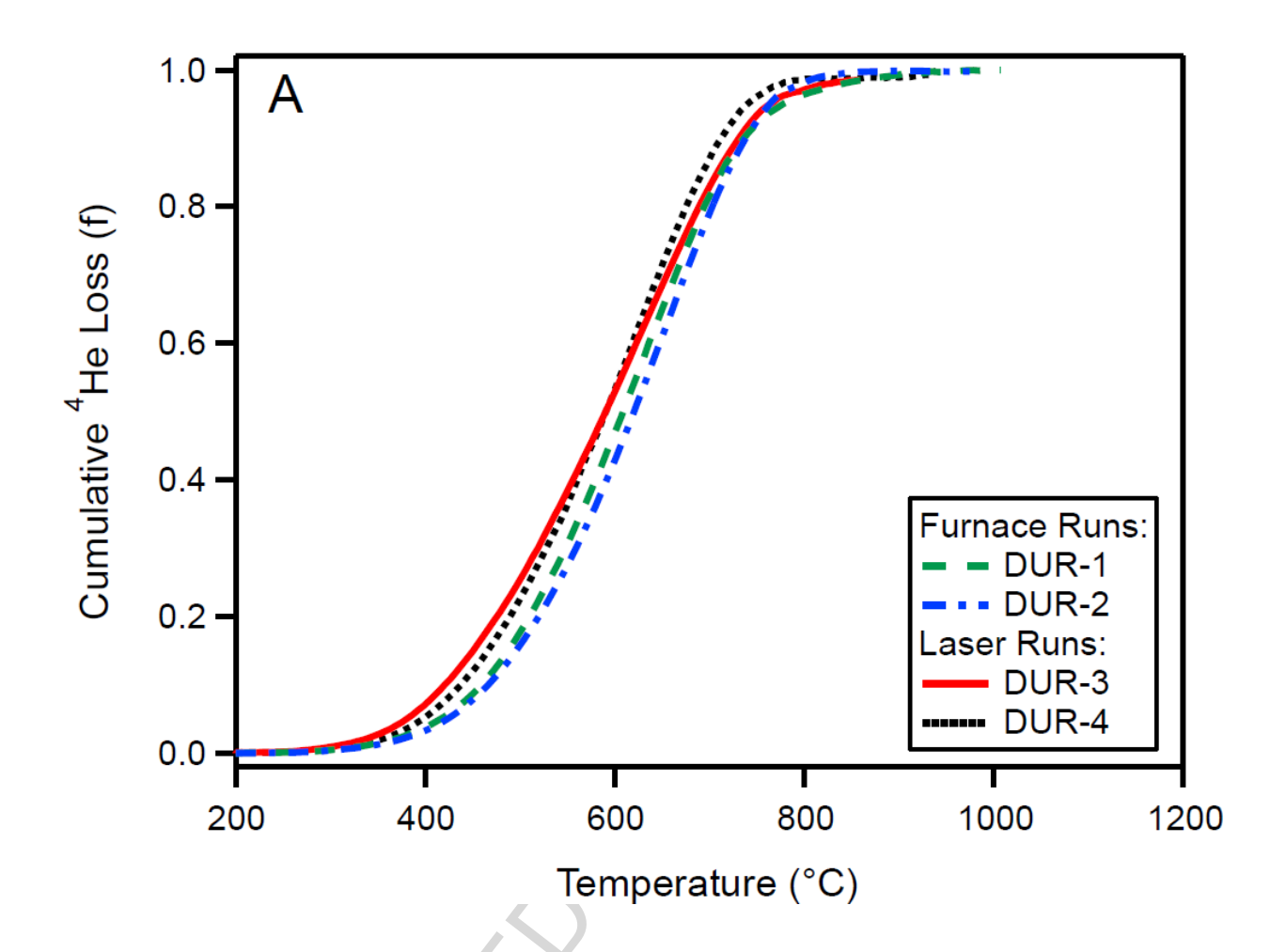


Fig. 4A

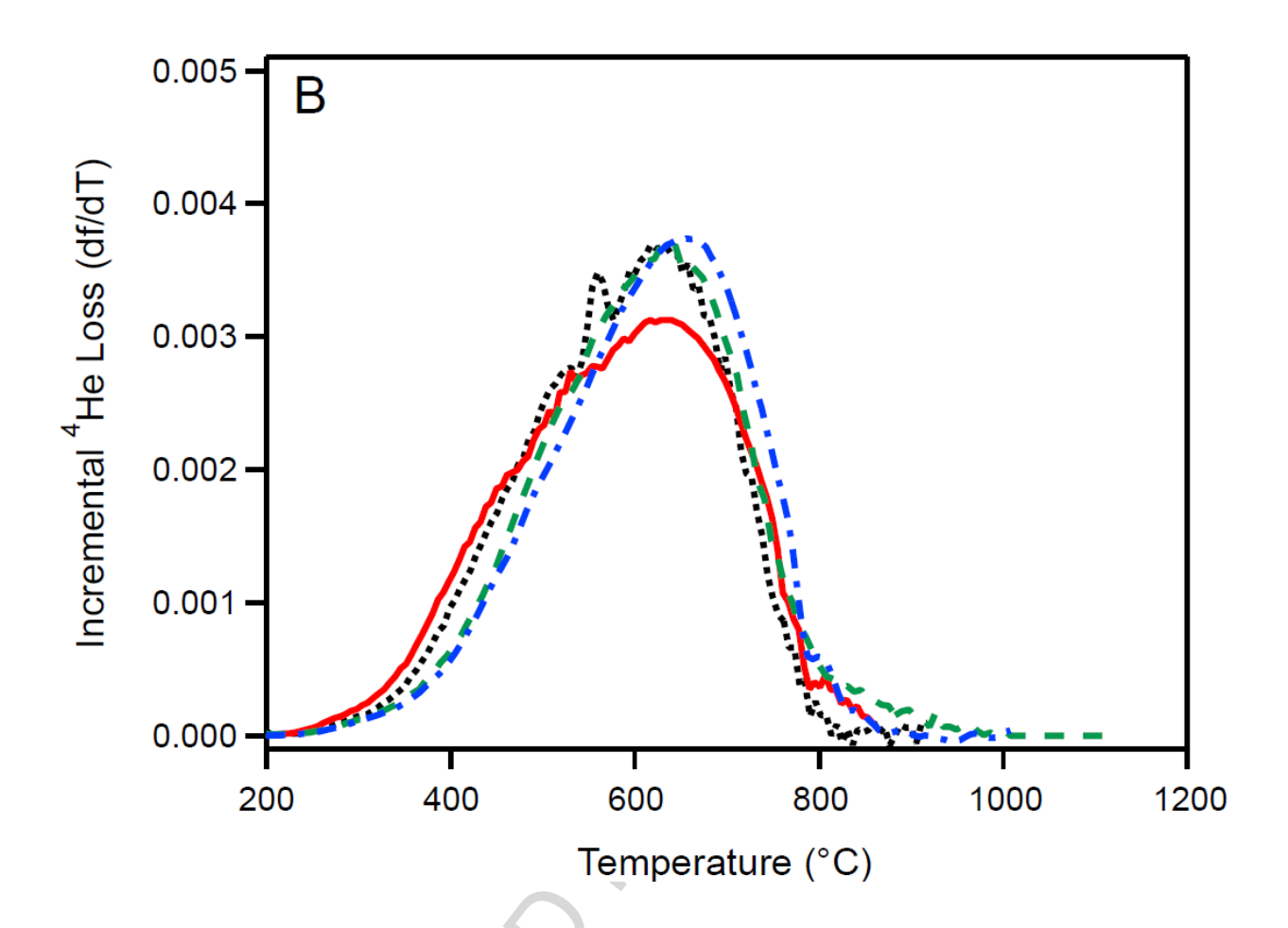


Fig. 4B

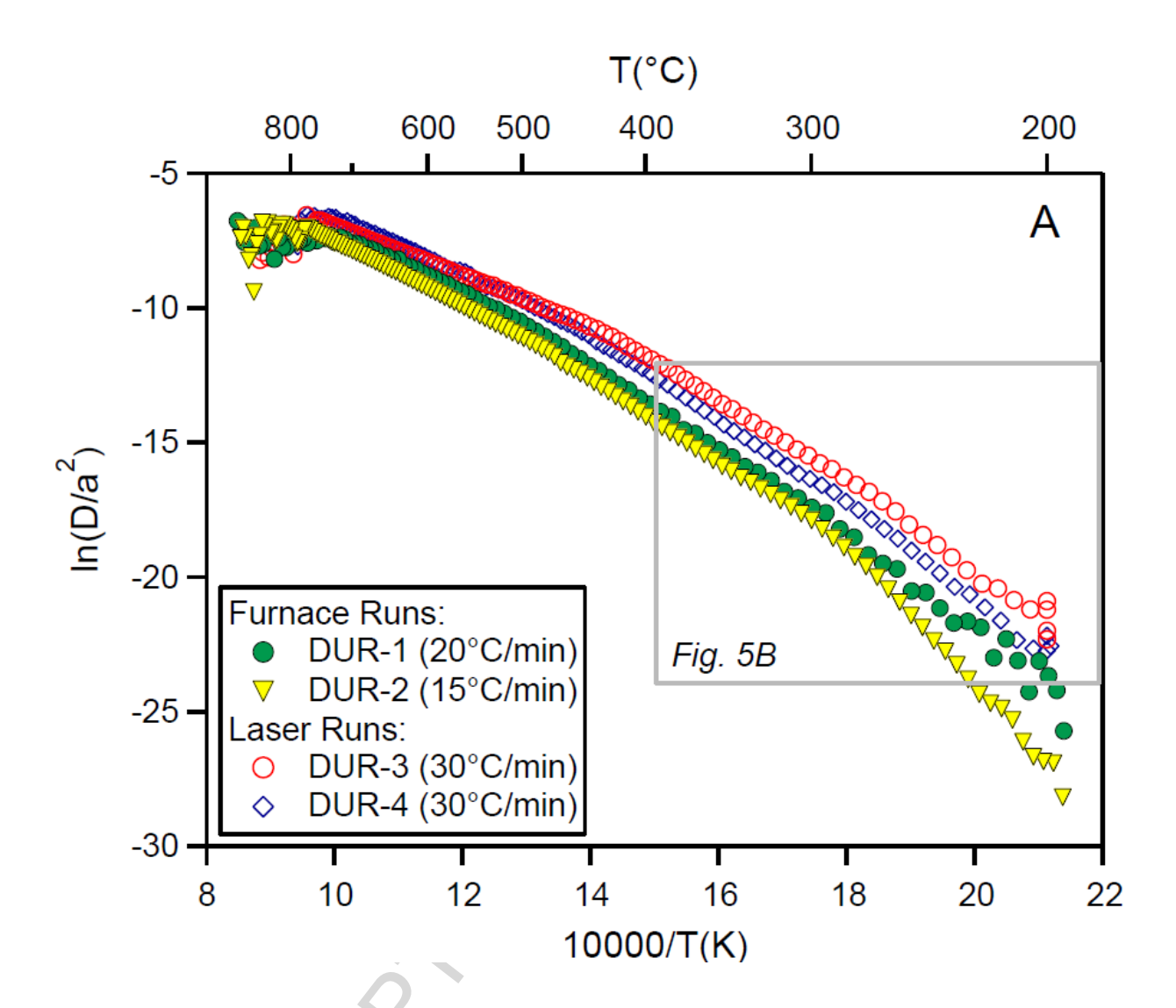


Fig. 5A

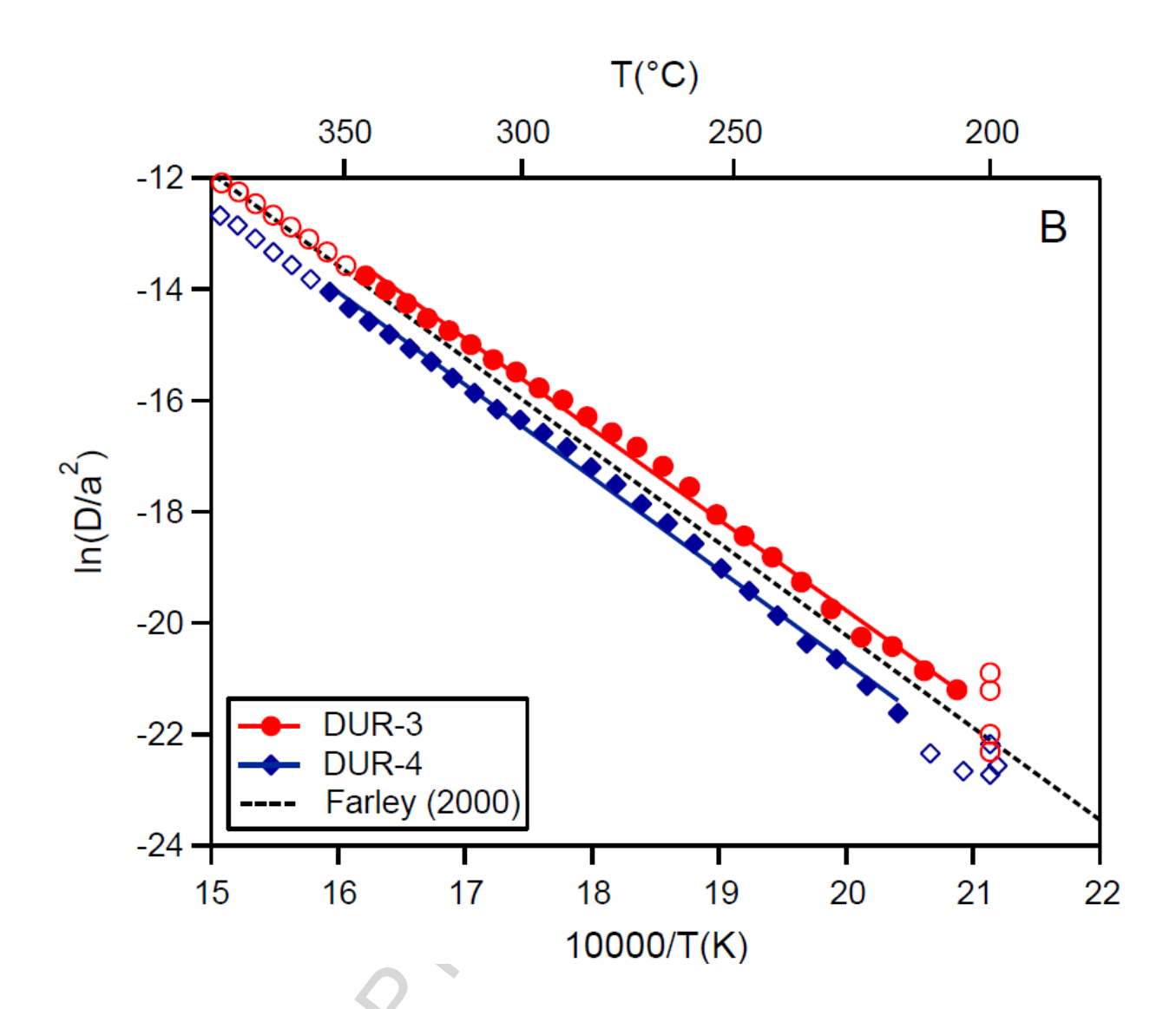


Fig. 5B

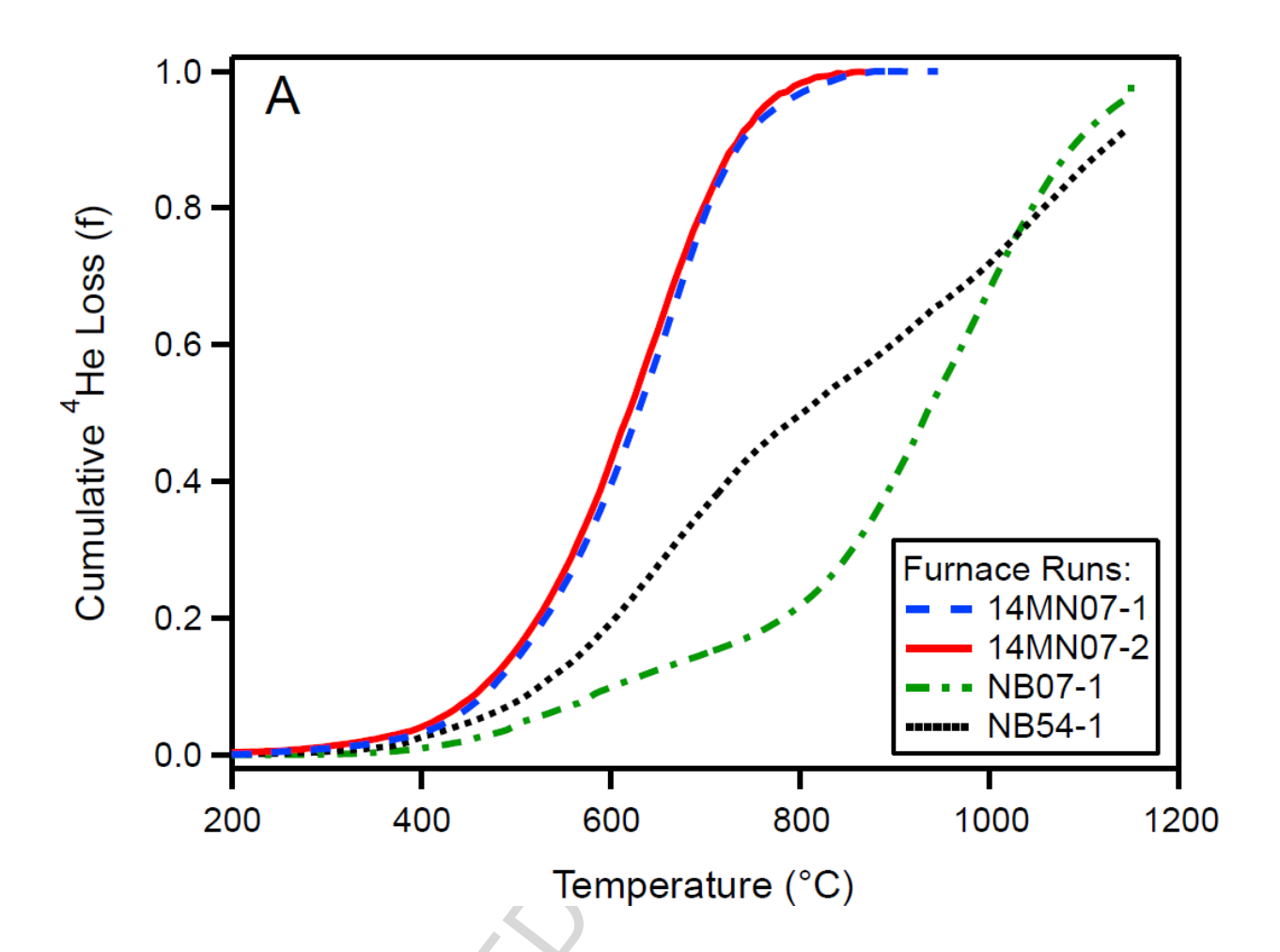


Fig. 6A

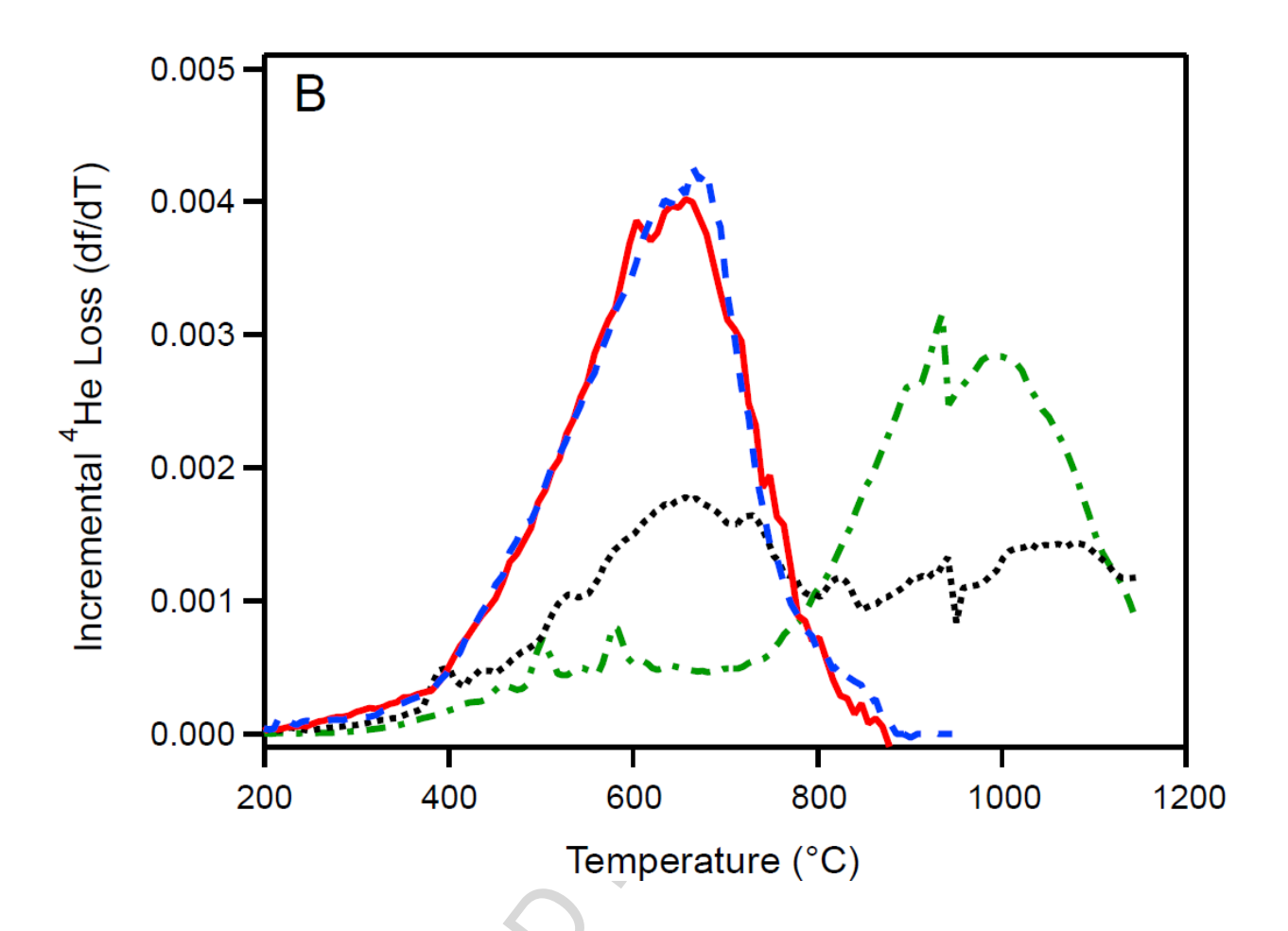


Fig. 6B